LARGE SCALE CONVECTION – OBSERVATIONS

How does the energy flow?

R.K. ULRICH
Department of Physics and Astronomy
University of California at Los Angeles

Abstract. Although the rate of production of nuclear energy in the sun's core almost certainly increases smoothly on time scales shorter than and comparable to the solar age, the mechanisms transporting this energy to the photosphere may be subject to more erratic fluctuations. Indeed space observations establish that the total solar irradiance in the direction of the earth is variable on time scales of days to years. I discuss energy transport by convection and magnetic fields with consideration of the possibility of energy storage through changes in the solar radius. Convection is the primary means of energy transport below the solar surface and must be involved in any modulation of energy flow. The large scale and long duration properties of solar convection arising from zones below the solar surface can be well studied using the Michelson-Doppler Imager instrument on SOHO. New evidence of long duration convective structures based on the MDI data is presented. These patterns appear to be related to the torsional oscillations observed at the Mt. Wilson Observatory.

1. Introduction

A major objective of solar physics is to understand the solar cycle. The roughly regular rise and fall of solar surface magnetic fields has a major impact on the earth's environment and could play some role in climate should the pattern undergo a change like that during the Maunder Minimum. While there has been progress in numerical modeling, the observational basis for our understanding of the fundamental mechanism of the solar dynamo has not progressed greatly. I have chosen to focus on this question rather than to prepare a comprehensive review of the literature. Much of the material from the Mt. Wilson synoptic program has not been previously presented.

I suggest that one approach worth exploring is to focus on the energetics of the dynamo. In human detective work a good plan is to follow the money trail. In solar detective work I think a similar good plan is to follow the energy trail. The forms of energy relevant to the solar interior and surface are nuclear, radiative, thermal,

F.-L. Deubner et al. (eds.), New Eyes to See Inside the Sun and Stars, 59–72.

gravitational, kinetic and magnetic. The core nuclear reactions are the starting point. The energy moves out to the convective envelope boundary in the form of radiation. These two steps probably do not play a role in the solar cycle of magnetic activity and I will say no more about them. Within the convective envelope, the matter is so opaque that radiative energy transfer can be neglected until the very surface layers are reached. The energy is carried through the convective envelope in the form of correlated thermal heat content of the matter and the vertical velocity of displacement. This process is known as convective energy transport and has been successfully modeled in the near-surface layers but is poorly known over the entire convective envelope. For the largest scales of motion, we can crudely estimate turnover times from mixing length theory (Vitense, 1953, Kim *et al.* 1996) and find they should be long compared to the rotation period. Consequently, there should be a strong interaction between rotation and convection. This is a case where thermal energy is converted by buoyancy into kinetic energy which then can interact with rotational kinetic energy. In addition, the magnetic energy somehow becomes coupled with the rotation and convection to generate the solar cycle. The entire problem is too much to address as a whole so I will focus on just two parts of the energy flow:

- What can we learn about large-scale and long-lived kinetic energy patterns in the sun's convective envelope?
- Does the variation in localized energy release associated with distinct surface activity cause a correlated change in the thermal or gravitational energy in the immediate subsurface regions?

Such storage would result in a change in the average density of the solar matter (see Spruit 1977, Fox and Sofia 1994). Although these calculations did not estimate the effect on the position of the solar surface, the alteration of the density suggests there should be an observable change in the solar limb figure. While I do not focus on the related magnetic energy questions, it is clear from the large scale velocity measurements presented below that pathways exist for the interconversion of magnetic and kinetic energy.

Our ideas about the sun's convection zone below the solar surface have been largely guided by general theoretical considerations (the mixing length theory of Vitense [1953] is usually a starting point) and numerical modeling experiments (see the recent discussion by Kim *et al.* [1996] for a comparison between mixing length theory and numerical simulations). Most of the unstable region is close to a polytropic structure. In such a region the temperature is roughly proportional to the distance below the solar surface. The pressure scale height is often taken as providing an estimate of the spatial scale of the convective flows. Because the pressure scale height is proportional to the temperature, it is also proportional to the depth below the solar surface. Thus general theoretical considerations lead us to believe there is a systematic increase in spatial scale of the convective flow as we look deeper below the surface. Similar ideas lead to the expectation that the convective velocity decreases inward below the surface boundary layer. Such simple arguments suggest that the convective cell or eddy lifetimes should range from about 10 minutes at the solar surface to in excess of one month near the inner boundary of the convection zone. At the inner edge of the convective envelope, the pressure scale height is a major fraction of the geometric separation between the inner and outer boundaries of the convection zone so we are led to believe that the largest scale convection currents could have a scale comparable to that of the convection zone as a whole. This general picture was originally introduced by Simon and Weiss (1968).

For the largest scale motions, it is clear that the influence of solar rotation will be dominant. These hypothetical convective flows are known as "giant cells" and have never been identified from solar observations. Theoretically one might expect there to be a wide range of spatial scales extending between the "giant cells" and the surface granulation. The only well accepted convective pattern between these two extremes is the supergranulation. However, the spatial scale of the supergranulation is not precisely defined and probably encompasses a range of sizes from the mesogranulation introduced by November *et al.* (1981) below 10 Mm to duragranulation discussed by Ulrich *et al.* (1998, see below) at 50 Mm.

Throughout the convection zone the requirement that the motions carry the energy flux imposes a limitation on the velocities achieved. In the deeper layers, the high density and high heat content per unit mass means that only a small velocity is needed to satisfy the flux requirement. Thus there is an inverse correlation between the spatial scale of the convective flow and the amplitude of its velocities. Unless some filtering technique is used, the smallest scale flows will dominate any velocity map. The larger scale flows can only be revealed by taking advantage of the short lifetime of the smaller scale patterns. Progressively longer temporal averaging intervals should reveal progressively larger scale flows. The granulation may be the dominant spatial scale of convection at the solar surface where we observe the interiors of the hot and cool flows. The spatial and temporal scales immediately larger and longer lived than the granulation cannot be observed easily due to the masking effect of the non-convective phenomenon of the five-minute oscillations. In practice filtering out the oscillations requires averaging over a time period of 20 to 60 minutes. Any convective pattern with a similar lifetime is also removed in this process. The convective pattern which remains is the "mesogranulation". Caution is required in identifying the "mesogranulation" since smaller scale motions are removed by the filtering process needed to suppress the oscillations.

In pushing the study of supergranulation toward larger scales it has been possible to obtain good isolation of these structures by using time sequences as long as possible. From ground-based facilities, it is difficult to obtain observed sequences with high temporal continuity for intervals longer than 14 hours. Supergranulation is the most prominent large scale flow on the solar surface and estimates of its lifetime are about 24 hours. The large amplitude five-minute oscillations impose another requirement on duration of observing sequences – they must be long enough that the oscillations can be averaged out. For convection patterns with lifetimes longer than the supergranulation, solar rotation becomes a major issue. Even a stationary velocity field will undergo apparent evolution due to the changing projection factors as the observed region is carried under the field of view. We do not have an option of observing from a heliostationary platform. This effect seriously compromises any effort to determine the lifetime of the velocity pattern using power spectral techniques. However, the changing projection angles can be used to determine both north-south and east-west velocities for the longest lived flows. The following section describes the implementation of this analysis.

Prior to the development of the methods of helioseismology, the solar surface was the only place where solar velocities could be observed. While the seismic observations can reveal properties of the internal flows, the deduction is difficult to carry out unless observations like those from the Michelson-Doppler Imager experiment on SOHO are available. These have good spatial resolution and during the dynamics program have good temporal continuity.

2. The Observed Velocity

2.1. NATURE OF THE OBSERVATIONS

Direct velocity observations can be made by way of the Doppler shift of spectral lines. Such observations provide only the line-of-sight component of the velocity and measure the apparent shift of some feature of a spectral line. Line shape and offset is influenced by unresolved convective effects as well as radiative transfer effects which depend on the center-to-limb angle ρ of the observed point. Such line shifts are generally referred to as the "limb shift". Differential solar rotation also enters into the apparent line-of-sight velocity as the largest effect and must be removed in order to make any large scale convective patterns apparent. The task of extracting appropriate deviations from the background differential rotation and limb shift functions may have a cross-talk effect in which spurious patterns are added or true patterns are removed. For the Mt. Wilson data the long duration of the observations permit a clean method of making the separation: the background functions are derived from observations prior to 1986 while the deviations are studied for observations after 1986. For the MDI data, Ulrich *et al.* (1998) have restricted the study to spatial scales small enough that the cross-talk problems are minimal.

The interpretation of the line-of-sight velocities in terms of long-lived flows must take into account the gross effect solar rotation has on the angle the line-of-sight makes with the solar surface. The continuously changing viewing angle causes even stationary flows to appear to vary. At each point within the solar atmosphere the stationary or long-lived velocity could have three components: vertical or radial, $V_{\rm r}$, horizontal east-west, $V_{\rm EW}$, and horizontal north-south, $V_{\rm NS}$. However, since I am primarily interested in the longest-lived and largest scale flows, I can use the small ratio of the vertical density scale height to horizontal structure size in the continuity equation to show that the ratio of horizontal velocity to the vertical velocity must be large. After ignoring the vertical velocity and following the formulation by Howard and Harvey (1970) I can express the line-of-sight velocity $V_{\rm los}$ as:

$$V_{\rm los} = V_{\rm EW} \cos B \cos B_0 \sin L + V_{\rm NS} \sin(B - B_0) \cos L \qquad (1)$$

where L is the central meridian angle of the point in question, B is the solar latitude and B_0 is the tilt of the sun's equatorial plane of rotation relative to our line of sight.

We now fix the background rotation by an external model $V_{\rm rot}$ and calculate a deviation of the line of sight velocity at each point according to:

$$\delta V_{\rm los} = (V_{\rm EW} - V_{\rm rot}) \cos B \cos B_0 \sin L + V_{\rm NS} \sin(B - B_0) \cos L - V_{\rm LS}(\rho) \qquad (2)$$

where $V_{\rm LS}$ is the limb shift velocity which is a function of center-to-limb angle ρ. We use the time dependence of $\delta V_{\rm los}$ which results from the regula r increase in L to determine both $(V_{\rm EW} - V_{\rm rot})$ and $V_{\rm NS}$ by fitting $\delta V_{\rm los}$ to the L dependence shown in equation (2). The dependence of $\delta V_{\rm los}$ on L is nearly linear with the slope giving the EW component and the intercept giving the NS component. Thus I can express the result of the fit in terms of a vector sum:

$$\boldsymbol{V} = (V_{\rm EW} - V_{\rm rot})\, \boldsymbol{i}_{\rm EW} + V_{\rm NS}\, \boldsymbol{i}_{\rm NS} \qquad (3)$$

where $\boldsymbol{i}_{\rm EW}$ and $\boldsymbol{i}_{\rm NS}$ are unit vectors parallel and perpendicular to the sun's equator. This vector $\boldsymbol{V}$ then gives both the direction and magnitude of the velocity deviation from strict differential rotation.

https://doi.org/10.1017/S007418090023831X Published online by Cambridge University Press

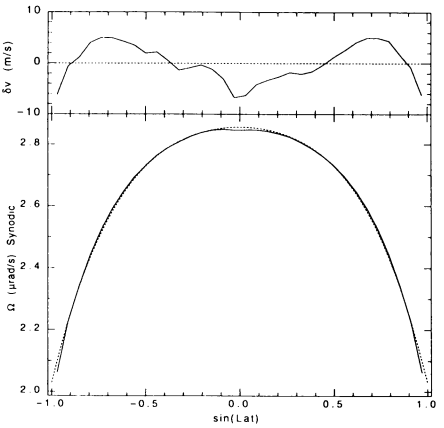

Figure 1. The reference rotation curve subtracted from all observations is shown as the solid line. For comparison the curve derived from the classical $\Omega = A + B \sin^2(\text{Lat}) + C \sin^4(\text{Lat})$ curve is show n as the dashed line. Note that while the curves are similar, there are small but significant deviations between the actual and the classical curve. The top panel gives the change in velocity implied by the difference between the two curves.

2.2. MT. WILSON VELOCITIES

The synoptic program at Mt. Wilson obtains solar magnetogram observations up to twenty times per day using the Babcock system established at the 150-foot tower. These data are observed using the light of the FeI line at λ525.02nm. The spectral sampling of this radiation utilizes fiber-optic image reformattors which select two nearly identical bands on opposite wings of the line. This selection has changed little after 1982. The passbands are characterized by two parameters: the full width of each, w, and the separation of their centroids, s. The detailed velocity and magnetic field values determined by a Babcock Magnetograph depend on these two parameters. There have been two changes since 1982 which have altered w and s: before Nov. 21, 1994 we used a grating having 632 lines/mm in 5th order and after that date we have been using a grating having 367.5 lines/mm in the 9th order. On the date of the change the fiber-optic reformattor was unchanged. Before the grating change the values of w and s were 6.21 nm and 7.76 nm respectively. After the change the values were 5.27 nm and 6.59 nm respectively. Beginning April 13, 1996 we have been using a 24-channel data system which incorporates new fiber-optic reformattors. With these new fiber-optics the values are 5.82 nm and 7.77 nm.

The large scale convective structures we seek may reveal themselves through their velocity variations. Herein comes the problem: a variation is a difference between a particular velocity measurement and some reference state — how do we identify the reference state? There is a temptation to assert that the reference state is defined by some particular combination of terms in a mathematical expansion; but without a physical theory which establishes the appropriate mathematical expansion any variations probably just indicate the inadequacy of the choice of mathematical terms. Our solution is to utilize a temporal average over more than one solar cycle for the reference state. An additional potential problem in the reference state definition is the possibility that any large transient feature could alter the reference state in such a way as to reduce the apparent size of the transient. We avoid this possibility by defining the reference state with data prior to our study period. This procedure gives us the reference rotation curve shown in figure (1) Although we begin our rotation rate analysis with the regular $\Omega = A + B \sin^2(\text{Lat}) + C \sin^4(\text{Lat})$ function, we apply a small correction to this function in order to properly represent the actual rotation rate averaged over the time period 1975 to 1986. The lack of symmetry between north

https://doi.org/10.1017/S007418090023831X Published online by Cambridge University Press

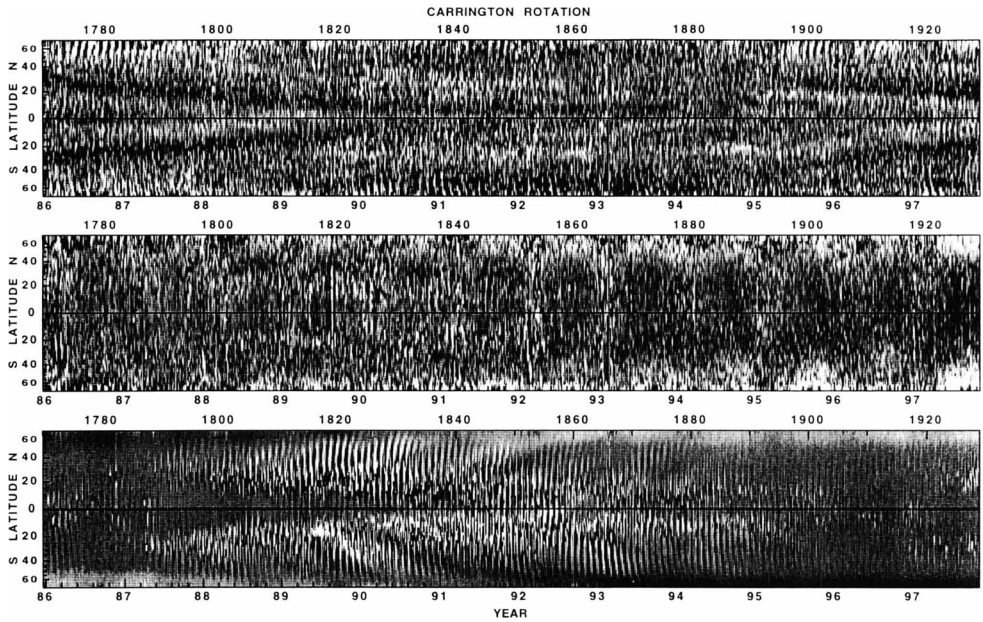

Figure 2. An eleven-year (1986 to 1997) record of the Mt. Wilson velocity and magnetic data showing the development of a full activity cycle. The top figure gives the deviation in rotation rate relative to the curve in figure (1) as a function of time and latitude. The grey-level for this panel is such that black represents 5 m/s faster than average rotation and white represents 5 m/s slower than average rotation. The middle panel gives the results for the north-south component of velocity. This motion mostly represents the meridional flow and is shown as a deviation from a long term average. For this panel white represents recession velocity and black represents approach velocity and the limits are again ±5m/s. The bottom panel gives the magnetic field with a saturation level of 2 gauss.

and south probably results from statistical fluctuations.

We display the magnetic fields and deviations in velocity from the reference state as defined by equation (3) in a format we term supersynoptic charts. A standard synoptic chart displays a full solar surface chart of magnetic field as a function of latitude and Carrington Longitude. The normal convention is to have East on the right and West on the left so that the points crossing the central meridian first are to the right and points crossing later are on the left. We reverse the order of the horizontal axis so the Carrington Longitude decreases from left to right. The advantage is that now time of central meridian passage increases from left to right and we may abut successive synoptic charts into long continuous chart where horizontal axis is the time of central meridian passage. By compressing this chart it can be reduced to a size where a very long time can be displayed compactly. Another format sometimes used to display long data sequences is called a stackplot. In a stackplot typically a range of latitude is selected and then the property as a function of longitude for successive Carrington rotations are plotted as strips above one another. These might be more precisely referred to as a latitude stackplot. One might also consider a longitude stackplot in which a band of longitude is selected and then the variable plotted in strips as a function of latitude for successive carrington rotations. Our supersynoptic

https://doi.org/10.1017/S007418090023831X Published online by Cambridge University Press

chart is a form of longitude stackplot except that all possible longitude strips are included.

In figure (2) the supersynoptic charts for V_{EW}, V_{NS} and B are shown on the top, middle and bottom panels. Owing to the fact that the east-west direction is parallel to the node lines in zonal harmonics and the north-south direction is parallel to node lines in sectoral harmonics, we refer to the top panel as the zonal flow map and the middle panel as the sectoral flow map. The Carrington Rotation number is shown along the top of each panel and this figure includes just over 150 rotations. Each equatorial circumference is divided into eight bins providing minimal resolution in this dimension. The most important results are contained in the top chart which shows the torsional oscillation and related velocity patterns. The middle chart which nominally should show variations in the meridional circulation rate in fact shows a long term trend which is not correlated with the solar cycle in a simple fashion and which may be a result of changes in the data taking system. Both velocity plots include a clear annual effect which is related to the reduced frequency of observation during the months of January to April. The feature which is most evident in the zonal flow map is the torsional oscillation first described by Howard and LaBonte (1980). The bands of faster than average rotation rate begin on the left edge of the map at about $\pm 30°$ latitude and reach near the equator by mid-1990. The analysis method we use provides considerable detail in the structure of this velocity pattern. Apart from a few periods during the southern California rainy season and the long term, large scale trends in the sectoral flow map, the structure shown in the two flow maps is of solar origin. The three successive winters from 1991 to 1993 provide clear examples of the nature of the maps when the data is inadequate.

Keeping the above limitation in mind, the following features can be summarized from the flow maps:

1. During the early part of the eleven-year cycle, the latitude where the zonal velocity has a well defined maximum, this latitude marks a lower boundary below which no substantial magnetic fields are found.
2. During the time around solar maximum, the torsional oscillation pattern is not well defined. A weak pattern at low to middle latitudes is present but it does not drift in latitude.
3. While there are periods when longitudinal structures appear to persist for more than a single rotation, in general such patterns are rare and not prominent. Those longitudinal structures which are present show significant changes from one rotation to the next.
4. Taking times of solar minimum to be 1986.6 and 1996.4, the early phase of the torsional oscillation pattern is much weaker for cycle 23 compared to the same phase of cycle 22. This is illustrated in figure (3) which shows the peak speedup velocity as a function of time for the two cycles. The southern hemisphere was weaker than the northern hemisphere after the pattern began to emerge in mid-1996.
5. The polar regions exhibit substantial changes in their average rotation rate. The south pole in particular for the period 1990.5 to 1994.5 showed this effect with an amplitude reaching 8 m/s.
6. For extended periods the polar regions show a pattern of rising and falling rotation rate synchronized to the polar rotation period. This pattern is largely along lines of constant solar longitude but is slightly tilted in a manner consistent with shear from differential rotation. In the 1986 to 1988 northern pole episode, a

pattern was also seen in the sectoral flow map in a phase consistent with the flow being a polar crossing sheet. In successive quarter rotations such a sheet flow carried with rotation has a sequence of apparent effects:

(a) First it appears to enhance rotation.

(b) One quarter rotation later it appears to be receding.

(c) In the third quarter it appears to diminish rotation.

(d) In the final quarter it appears to be approaching.

The sequence observed is consistent with this pattern.

7. For several periods the torsional oscillation pattern contains structures which persist more than one rotation. These are most evident in 1986 and 1996 prior to the onset of solar activity. These have sizes comparable to the solar circumference and would be described by low degree spherical harmonics.
8. Although the polar speedup and the remnants of the equatorial faster- than-average zone are present in 1991 to 1994.5, the torsional oscillation pattern does not seem to be connected as a single and unified phenomenon. Rather the torsional oscillation seems to precede the onset of activity at the beginning of the cycle and govern its initial migration toward the equator. During the declining part of the cycle the pattern does not seem to be related to the activity.
9. The magnetic field reversal occurs at the time when the polar speedup is most evident. During this period the fluxtubes associated with the decaying active regions are being swept toward the poles by the meridional circulation. Such fluxtubes could be aligned radially and provide a coupling between the more rapidly rotating interior at lower latitudes and the more slowly rotating polar regions. Thus the polar speedup may be a consequence of this coupling. The polar crossing flows are also evident during these periods and could be a consequence of unbalanced torques produced by the fluxtubes.

The representation given in figure (2) contains more information than is necessary to illustrate the torsional oscillations. If, instead of dividing each Carrington rotation into eight latitude bins, we use just one, the structures are smoothed out leaving only the longitude dependence at a lower velocity amplitude. The resulting figure (3) shows the migration of the torsional oscillation pattern very clearly. While the equatorward drift of the latitude of rotation rate increase is easily seen during the early years of the cycle, the pattern reaches the equator after only about 5 years of the cycle and then remains at a nearly fixed latitude while gradually weakening. During the final three years of cycle 22, the pattern was nearly absent. The relationship between the polar speedup noted above and the later torsional oscillation is unclear. If the speedup had drifted equatorward following the appearance at the polar regions to join the subsequent mid-latitude torsional pattern, it would have been easy to associate the two phenomena as part of an extended solar cycle. Instead with the several-year gap, the connection is less clear.

The grey-level plots of figures (3) and (2) provide a good representation of the evolution in two dimensions but are difficult to compare quantitatively. To facilitate such comparisons, I have averaged the rotation rate over three successive rotation periods. The results of this procedure are shown in figure (4). Each average deviation curve is displaced vertically by an increment of 5 m/s. The central time for the average is given to the right of each line. The left-hand panel shows the result for solar cycle 22 and the right for the early part of solar cycle 23. The migration of the maximum is quite evident.

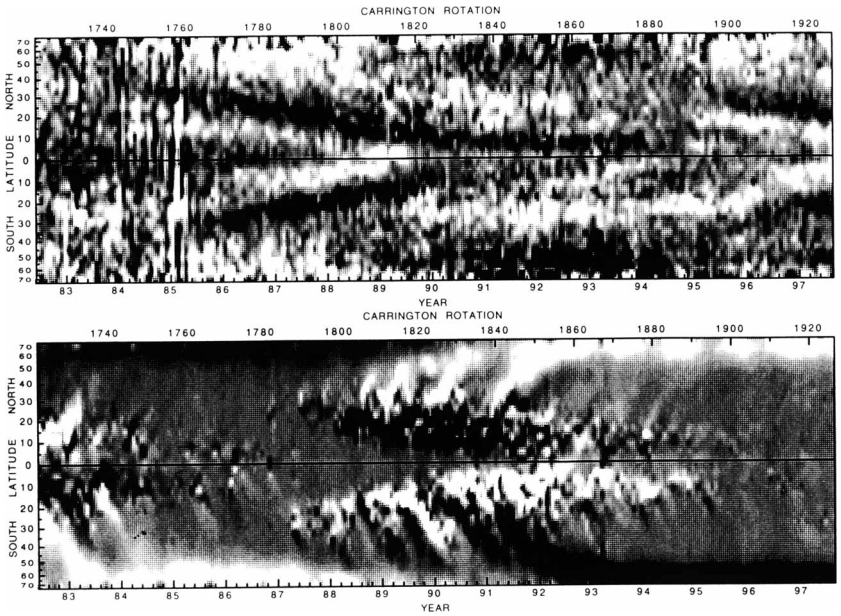

Figure 3. The torsional oscillations averaged over the solar circumference. The top panel gives the zonal velocity and the bottom panel gives the average magnetic field. The zonal velocity is coded in grey level such that white represents 3 m/s less than average rotational velocity and black represents 3 m/s faster than average rotational velocity. The magnetic field, also averaged over the circumference is indicated by black/white saturation of ±0.75 gauss.

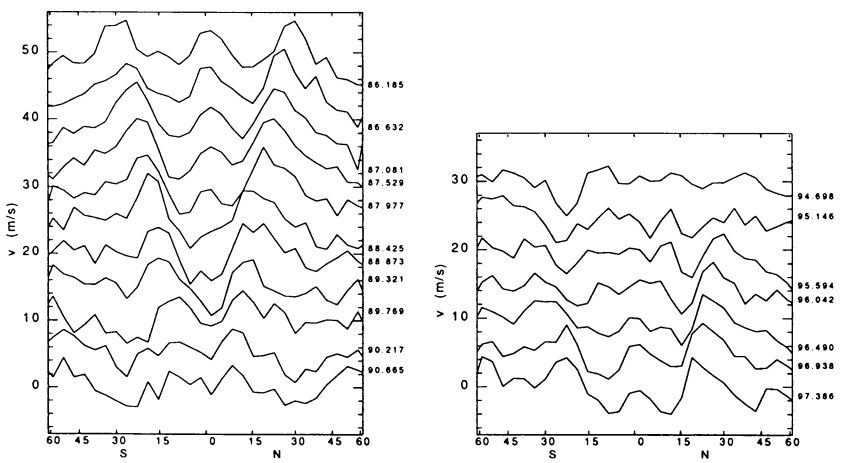

Figure 4. The change in rotation rate averaged over three successive Carrington Rotations for specified time intervals near the beginnings of solar cycles 22 and 23. Each line gives this average and is offset from zero velocity by an integer multiple of 5 m/s. The time in years at the center of the averaging interval is indicated to the right of each line. These results are only shown near the beginnings of each cycle where the pattern is well defined.

https://doi.org/10.1017/S007418090023831X Published online by Cambridge University Press

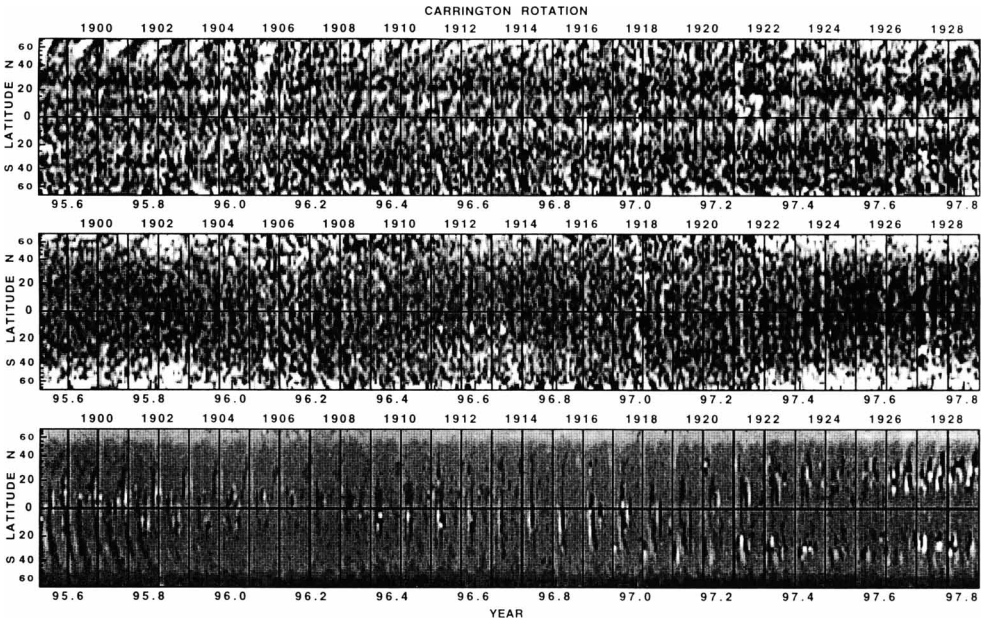

Figure 5. The zonal flow map for the past two years together with the sectoral flow map and the magnetic field map. In this figure each Carrington Rotation boundary is indicated by a vertical line.

The helioseismic analysis of observations from the MDI instrument on SOHO now makes it possible to obtain regular observations of the torsional oscillation pattern with another system (see Schou *et al.* in these proceedings). To facilitate comparison of these new results with the evolution of the torsional oscillation pattern, I include here as figure (5) a magnified version of figure (2) for just the past two years.

An important question to be applied to data such as shown in figures (2) and (5) is whether there are velocity structures of very large scale which persist over more than one solar rotation. The statistics of the flow maps are difficult to define because of the substantial noise which is present each winter. There are however hints of repeating patterns. The maps shown in figure (5) are best suited for this examination. Here as in figure (2) the polar crossing flows are most evident after mid 1995 in the north polar region. On the sun's equator, there is a zone of faster than average rotation rate which coincides with Carrington longitude 0° lasting from CR1919 to CR1922. At the latitude of the northern faster-than-average zone, there is a longitude about 330° (recall that the Carrington Longitude at the central meridian decreases with time) of faster-than- average rotation rate which is evident from CR1912 to CR1913. These features produce peaks at frequencies $\nu = m/\text{Rot. Per.}$ which are evident for $m \leq 8$.

2.3. MDI VELOCITIES

The data from the MDI instrument on SOHO provides an opportunity to study the solar velocities without any temporal gaps. During the dynamics program period (see Scherrer *et al.* 1995 for a description of the MDI instrument and programs) full disk

https://doi.org/10.1017/S007418090023831X Published online by Cambridge University Press

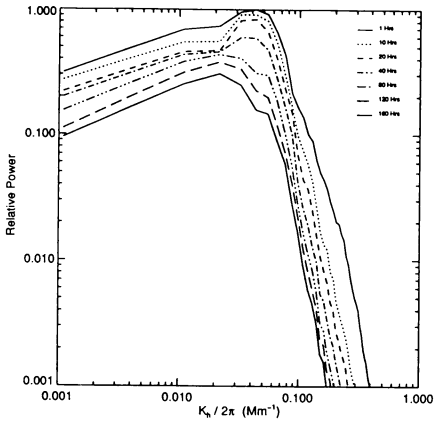

Figure 6. The spatial power spectra averaged over all azimuthal directions as a function of the inverse of the horizontal wavelength $K_h/2\pi$. Averaging periods for the curves from top to bottom are 1, 10, 20, 40, 80, 120 and 160 hours. The power is normalized relative to the maximum for the 1 hour averaging period. These curves are the average of the results for all eight study areas.

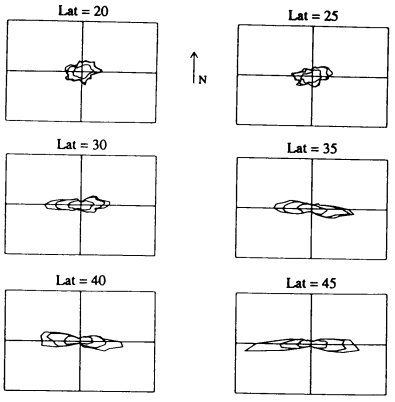

Figure 7. Windsock diagrams for six of the eight study areas from Ulrich *et al.* (1998). These represent the asymmetry of the velocity distribution as a function of the azimuthal angle relative to the local NS direction. Each contour is the average $|V|$ in the direction relative to the crossing point of the vertical and horizontal lines. The three contours are for all velocities less than 200 m/s, 300 m/s and no upper limit. The vertical axis represents ± 2 m/s.

velocity images made up of 2 arcsec square pixels are available for periods up to 60 days. Solar rotation prevents the continuous observation of any part of the solar surface for longer than about 180 hours. Although a part of the surface can be seen longer than this, the foreshortening outside of the 180-hour window is too severe to permit the kind of analysis necessary to study surface dynamics. Beck (1996) and Ulrich *et al.* (1998) have extracted from the MDI dynamics program images a sequence of 176 hours and carried through an analysis similar to that used for the Mt. Wilson velocities. Due to the high duty cycle for the MDI instrument and the absence of atmospheric disturbances, this data set yields a much cleaner set of velocity maps for both the NS and EW components than is available from the ground-based observations. A full discussion of these results is given in Ulrich *et al.* (1998). Here I summarize the principal results.

An important question is the temporal decay of the velocity field. Solar rotation makes this question difficult to analyze due to the changing projection angle. We extract the NS velocity component from the full images by averaging together images which are symmetrically placed relative to the central meridian thereby canceling the EW component. By extending the total time interval included in the average, we isolate the time decay of the NS component alone. The spatial power spectra as a function of this averaging interval is shown in figure (6). Note the initial rapid decay followed by a more gradual shift toward longer wavelengths. The decay at long averaging times is sufficiently slow that we believe there is a good chance the features persist for more than one rotation.

The full maps include both components of velocity and allow Ulrich *et al.* (1998) to study the isotropy of the flows. Each horizontal velocity vector defines an ampli-

https://doi.org/10.1017/S007418090023831X Published online by Cambridge University Press

tude and an azimuth angle relative to the local North direction. The isotropy can be quantified in terms of these azimuth angles by dividing the possible 360° into bins and calculating the average of the absolute values of the velocity vectors which fall into each bin. This produces what Ulrich *et al.* (1998) referred to as a windsock diagram after the patterns given for airplane pilots to evaluate the prevailing winds near an airport. Windsock diagrams have been calculated by Ulrich *et al.* (1998) for each of the eight study areas and are shown in figure (7) for six of these. The two areas nearest the equator are not reliable due to a contribution from vertical velocities. Most striking in figure (7) is the progressive domination of the EW velocities. In addition the peak of asymmetry lies along a line which deviates slightly from the EW direction. The sense of the deviation is that the faster than average vectors systematically move toward the equator and the slower than average vectors systematically move toward the pole. This effect has been found in the motion of sunspots (Ward 1965, Gilman and Howard 1984) but never before in the kinematics of velocity vectors for the gas. This tilt of the windsock diagrams at mid-latitude could be a direct indication of the process which maintains the solar differential rotation.

3. Energetics

The rise and decline in the strength of the sun's magnetic field is the major component in the modulation of the flow of energy from the interior to space. Throughout most of the interior, the magnetic energy density is far less than the kinetic energy of the convecting and rotating gases. Consequently, the dynamics of the convective envelope ultimately govern the dynamo process. However, even though the magnetic field is weak overall, it must be capable of modifying the dynamic flow through the weak effects of the magnetic forces. Based on these ideas, it is commonly assumed that the differential rotation is a consequence of the occurrence of a convecting fluid in a rotating, self-gravitating body. Numerical models (see Gilman 1980, 1992 for reviews) support this interpretation. The Ward (1965) correlation between NS and EW velocities would support the existence of differential rotation, and the determination from the MDI observations that this correlation is present in non-magnetic regions indicates that it can indeed lead to the existence of the differential rotation. Gilman (1980) suggests that the kinetic energy in the differential rotation is comparable to the convective energy. A critical question is the balance between the rotational and convective influences. When rotation dominates, the rotation tends to be constant on cylinders. The results from helioseismology show (Korzennik 1990, Kosovichev *et al.* 1997) that the rotation rate increases inward near the surface as if the radially moving currents were preserving angular momentum, then the rotation rate decreases inward as is required by the constant rotation rate on cylinders model. Perhaps this composite behavior is a result of a variable balance between rotational energy and convective kinetic energy with the former dominating in the deepest parts of the convective envelope and the latter dominating near the surface.

Superimposed on the differential rotation pattern are the solar cycle correlated velocity variations of which the torsional oscillation discussed above is the only phenomenon identified. While it has been suggested that the motion is generated by surface Lorentz forces (Schüssler [1981], Yoshimura [1981]), rough calculations based on this model (Rüdiger *et al.* [1986]) yield phasing inconsistent with the observations. The faster-than average band is observed to be closer to the equator than ±35° latitude and reaches the equator about at the time of maximum activity. For most

of the cycle, there is no clear evidence of two bands of faster-than-average rotation co-existing in either the north or south hemisphere. None of the Rüdiger *et al.* (1986) models show this single mode behavior and the one which comes closest has the faster-than-average band reaching the equator at sunspot minimum. Furthermore, these models require an interaction between a weak poloidal field and electrical currents generated by the deep toroidal field which is the ultimate source of sunspots and active regions. Current ideas about the solar dynamo place the toroidal field below the convective/ radiative boundary and it is unclear that the generated currents can persist to the solar surface.

The torsional oscillations occur both with and without any surface magnetic field. The pattern was clearly present through the minimum between cycles 21 and 22 but underwent a period of absence between cycles 22 and 23. The close association between the latitude of maximum speedup of rotation and the equatormost location of the magnetic fields indicates that the torsional oscillations are intimately connected with the dynamo. As the most evident large-scale velocity feature associated with the solar cycle, they represent the most significant kinetic energy component which is part of the solar cycle. The recent finding by Schou (these proceedings) that the torsional oscillations can be detected in horizontal velocity maps deduced from solar p-modes indicates that they are not confined to the solar surface. Snodgrass (1988) and Gilman (1992) suggest that they could be a consequence of Parker's (1987) "thermal shadow" effect. In this model the toroidal fields serving as the source of the activity block the flow of energy from the interior and produce a cool overlying layer which systematically induces downflows over a broad area. The coriolis force on matter flowing into the downflow region causes the poleward slower-than-average rotation and the equatorward faster-than-average rotation. Such behavior is seen in figure (3) in the northern hemisphere during the interval 1986 to 1992. The most recent pattern has the slower-than-average band equatorward of the faster-than-average band and only a weak indication of a poleward component.

The original title of this paper (assigned by the organizing committee) included the solar radius. I have been silent on this question because there is almost no data which can be brought to bear on it. It is a difficult observational task, probably requiring a space-based instrument. Brown and Christensen-Dalsgaard (1998) report tight limits on the possible variation of the sun's radius as defined by a parameter dependent primarily on the hydrostatic structure. Ulrich and Bertello (1996) using radiation emitted near the temperature minimum found a correlation in radius change and the solar cycle with an amplitude of 400 milli-arcsec (approximately two pressure scale heights). This latter result may due to a change in the average structure of the solar atmosphere. The energetic implications of these radius variations are unclear. Blocking or enhancement of the local rate of energy flow could produce a variation in the thermal energy of the underlying convective region and cause a change in the average volume and radius. Such an effect would be limited to a portion of the solar surface where the blocking or enhancement has occurred. Since the Brown and Christensen-Dalsgaard (1998) observations are derived from EW drift of the solar image across the detector, any high latitude bumps or valleys would not have been detected.

If Parker's "thermal shadow" effect is associated with the torsional oscillations, it might produce a zone of cooler-than-average material which could influence the overlying solar figure. A careful study of the time dependence of the solar figure might reveal such a depressed zone. However, the underlying zone of enhanced magnetic field could have the opposite effect of increasing the average radius. In addition,

atmospheric effects associated with surface activity on the overlying solar surface can also increase the apparent radius. This last source of confusion could be removed through the use of observations in the solar continuum and in spectral lines since the effect should be enhanced for the lines.

As a potential means of probing the energy flow through the convective envelope, observations of the solar figure carry great promise. Unfortunately, such observations are extremely difficult through the earth's atmosphere and are only now becoming available from space. Consequently, this portion of the paper remains a "wish list" rather than a report of results.

Acknowledgments: The long-term synoptic Mt. Wilson program has received support over the time interval shown in figure (3) from a variety of agencies including: US Government agencies NASA, ONR and NSF through a number of grants programs and by the Carnegie Institute of Washington. The acquisition and analysis of the MDI data has been made possible by support of the SOI Team at Stanford University which operates the MDI instrument, a NASA sponsored experiment on the ESA/NASA SOHO mission.

4. References

Beck, J.G. 1997, *Velocity Fields on the Solar Surface with Time Scales up to 30-Days*, PhD Thesis UCLA.
Brown, T. and Christensen-Dalsgaard, J.: 1998, *Astrophys. J.* Submitted.
Fox, P.A. and Sofia, S.: 1994, in J.M. Pap, C. Fröhlich, H.S. Hudson, S.K. Solanki (eds.), *The Sun as a Variable Star Solar and Stellar Irradiance Variations*, Cambridge Univ. Press, p. 280.
Gilman, P.A.: 1980, in D.F. Gray and J.L. Linsky (eds.), *Stellar Turbulence*, Lecture Notes in Physics, 114, Springer-Verlag, p. 19.
Gilman, P.A.: 1992, in K.L. Harvey (ed.), *The Solar Cycle*, ASP Conf. Vol. 27, p. 241.
Gilman, P.A. and Howard, R.F.: 1984, *Solar Phys.* **93**, 171.
Howard, R. and Harvey, J.: 1970, *Solar Phys.* **12**, 23.
Howard, R. and LaBonte, B.: 1980, *Astrophys. J.* **239**, L33.
Kim, Y.-C., Fox, P.A., Demarque, P. and Sofia, S.: 1996, *Astrophys. J.* **461**, 499.
Korzennik, S. 1990, *Helioseismic Observations from Mt. Wilson*, PhD Thesis, UCLA.
Kosovichev, A.G., *et al.* : 1997, *Solar Phys.* **170**, 43.
November, L., Toomre, J., Gebbie, K. and Simon G.: 1981, *Astrophys. J.* **245**, L123.
Parker, E.N.: 1987, *Astrophys. J.* **321**, 984.
Rüdiger, G., Tuominen, I., Krause, F. and Virtanen, H.: 1986, *Astron. Astrophys.* **166**, 306.
Scherrer, P.H. *et al.* : 1995, *Solar Phys.* **162**, 129.
Schussler, M.: 1981, *Astron. Astrophys.* **94**, L17.
Simon, G.W. and Weiss, N.O.: 1968, *Z. Astrophys.* **69**, 435.
Snodgrass, H.B.: 1988, in P.F. Schewe (ed.), *Phys. News in 1987*, AIP Special Report, p. S-11.
Spruit, H.C.: 1977, *Solar Phys.* **55**, 3.
Ulrich, R.K., Beck, J., Hill, F. and Bogart, R.: 1998, *Astrophys. J. Letters* Submitted.
Ulrich, R.K. and Bertello, L.: 1995, *Nature* **377**, 214;.
Vitense, E.: 1953, *Z. Astrophys.* **32**, 135.
Ward, F.: 1965, *Astrophys. J.* **141**, 534.
Yoshimura, H.: 1981, *Astrophys. J.* **247**, 1102.